THE JOURNAL OF PHYSICAL CHEMISTRY B

Article

pubs.acs.org/JPCB

Molecular Insight into Affinities of Drugs and Their Metabolites to Lipid Bilayers

Markéta Paloncýová, Karel Berka,* and Michal Otyepka*

Regional Centre of Advanced Technologies and Materials, Department of Physical Chemistry, Faculty of Science, Palacký University Olomouc, tř. 17. listopadu 12, 771 46, Olomouc, Czech Republic

Supporting Information

ABSTRACT: The penetration properties of drug-like molecules on human cell membranes are crucial for understanding the metabolism of xenobiotics and overall drug distribution in the human body. Here, we analyze partitioning of substrates of cytochrome P450s (caffeine, chlorzoxazone, coumarin, ibuprofen, and debrisoquine) and their metabolites (paraxanthine, 6-hydroxychlorzoxazone, 7-hydroxycoumarin, 3-hydroxyibuprofen, and 4-hydroxydebrisoquine) on two model membranes: dioleoylphosphatidylcholine (DOPC) and palmitoyloleoylphophatidylglycerol (POPG). We calculated the free energy profiles of these molecules and the distribution coefficients on the model membranes. The drugs were usually located deeper in the membrane than the corresponding metabolites and also had a higher affinity to the membranes. Moreover, the behavior of the molecules on the membranes differed, as they seemed to have a higher affinity to the DOPC membrane than to POPG, implying they have different modes of action in human (mostly PC) and bacterial (mostly PG) cells. As the xenobiotics need to pass through lipid membranes on their way through the body and the effect of some drugs might depend on their accumulation on membranes, we believe that detailed information of penetration phenomenon is important for understanding the overall metabolism of xenobiotics.

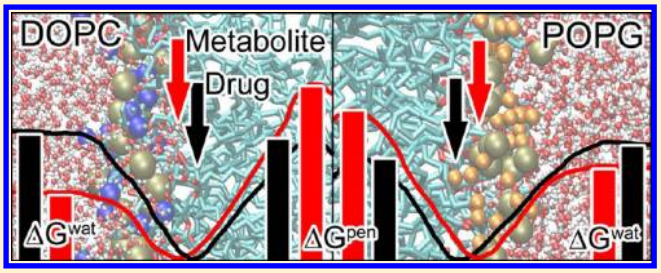

INTRODUCTION

The interaction of drugs with cell membranes dictates their pharmacological properties because it affects the drug distribution, transport, accumulation, partitioning, and metabolism.[1−5] A drug must be passively[6] or actively[7−9] transported across the cell membrane before it can reach its target and perform its biological role. Passive transport depends on membrane structure, dynamics,[10] and its permeability for a particular substance.[6] Recently, we suggested that the positioning of drugs on lipid bilayers might also affect their interaction with drug metabolizing cytochrome P450 (CYP) enzymes,[4] which are anchored to the membrane of the endoplasmic reticulum,[11] and as a consequence affect the metabolism of drugs. In addition, the positioning on and affinity to a membrane may play an important role in other biologically significant processes, such as antioxidant inhibition of lipid peroxidation.[12] The importance of drug−membrane interactions in biology, pharmacology, and medicine has called for extensive research in this field, which is rather challenging due to the complexity of biological membranes. Many experimental and theoretical techniques have been developed to study various aspects of drug membrane interactions.[1,13−16]

Cell membranes form a protective wall around the cellular interior against an external environment, and separate cytosolic and noncytosolic sides of organelles.[17,18] The membranes are predominantly composed of lipids, which form a lipid bilayer. Lipid bilayers are widely used as a membrane model in both experiments and theoretical calculations. The membrane compositions of various cell structures differ, and their properties are mostly determined by their lipid composition,[19] which is highly variable and includes numerous lipid types. However, by careful choice of lipid, a bilayer composed of one lipid type can mimic the key physicochemical features of a particular membrane.[1] In the present work, we chose to use a dioleoylphosphatidylcholine (DOPC) bilayer because phosphatidylcholine makes up about 40% of the human endoplasmic reticulum membrane mass,[19] where the drug metabolizing CYP enzymes are mostly located.[20] The other model, a palmitoyloleoylphosphatidylglycerol (POPG) lipid bilayer, was chosen as an example of a negatively charged membrane, which is typically present in bacteria.[21] Both bilayers differ in headgroup charge, density, thickness, and many other properties (Figure 1). Knowledge of the differences in cell membrane compositions among organelles or various organisms (e.g., between host and pathogen) can be used in rational drug targeting.[1] However, to exploit such information, the nature of drug−membrane interaction needs to be understood in detail.

Molecular dynamics (MD) simulation is a unique technique used in recent years for studying the dynamics of biological systems, simultaneously enabling fine space (atomistic) and

Received: November 30, 2012
Revised: February 6, 2013
Published: February 6, 2013

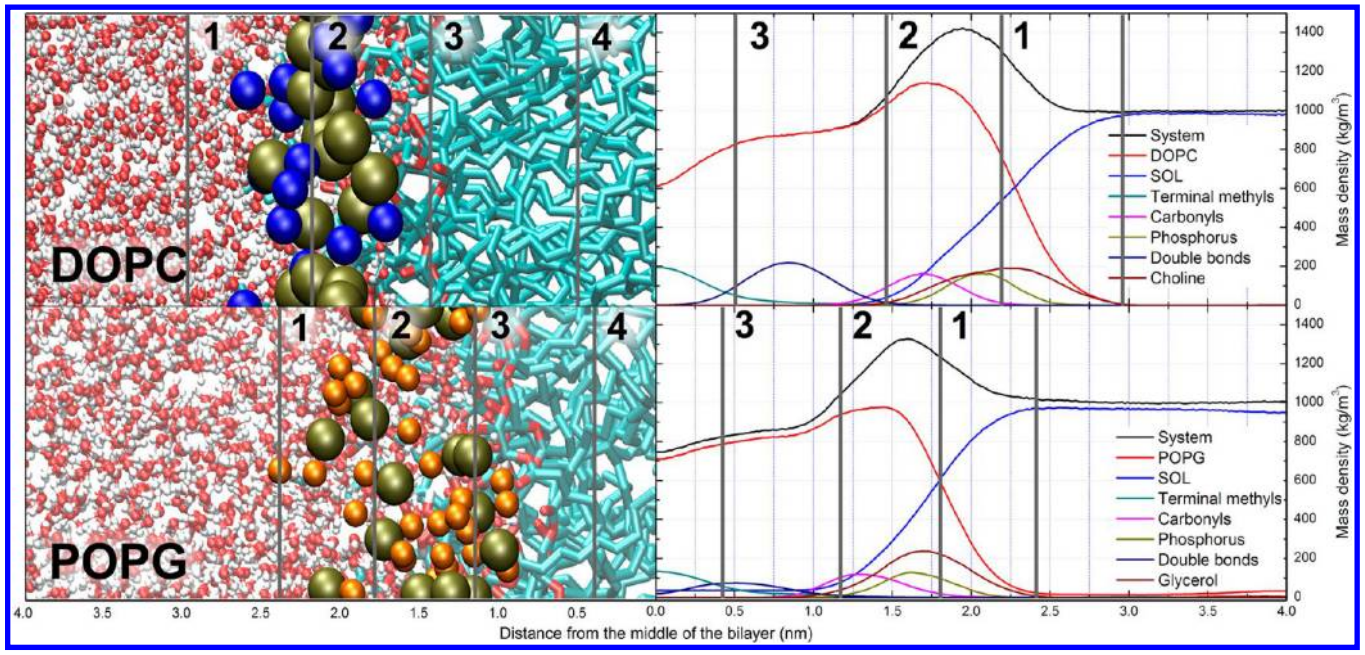

Figure 1. Lipid bilayers of DOPC and POPG analyzed in this study (left) and the density profiles of specified groups (right). The structure of the bilayer is divided into regions according to Marrink's four region model:[22] Region 1 — low density of head groups. Polar area, where the conditions are similar to bulk water, ends when the density of water (SOL) and head groups are comparable. Region 2 — high density of head groups. Bulk-like water disappears; this region ends when the density of water is below 1%. Polar molecules are usually located here. Region 3 — high density of acyl tails. Double bonds in unsaturated lipids are located here. Region 4 — low density of acyl tails. The overall density drops and the movement of molecules is usually quicker. Regions 3 and 4 usually form a barrier for polar molecules. Carbon lipid tails are represented by cyan sticks, phosphates are depicted as olive and nitrogens as blue balls, terminal glycerol oxygens in POPG head groups are orange balls, and water molecules are represented by red and white balls.

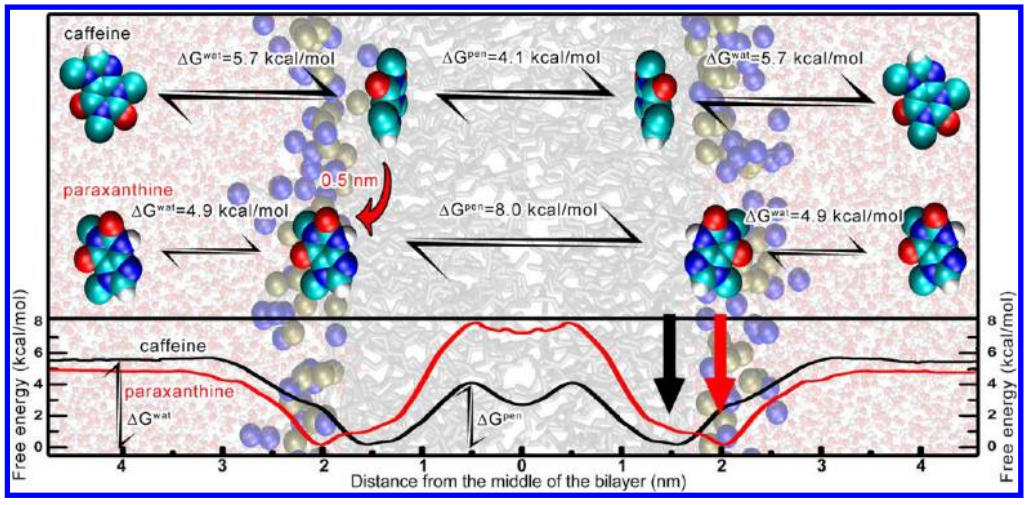

Figure 2. Scheme of caffeine and paraxanthine (caffeine metabolite) molecules moving through the DOPC bilayer (upper panel) highlighting the studied properties. The water/lipid barrier ΔG^{wat} of the drug (here caffeine) is higher than the corresponding value for the metabolite (paraxanthine), whereas the bilayer center penetration barrier ΔG^{pen} is higher for the metabolite. The position of the metabolite is located further from the bilayer center close to the polar headgroup region. The drug enters the membrane spontaneously and concentrates in the region near the entrance of the cytochrome P450 (CYP) active site access tunnel. The drug is metabolized in the active site and leaves CYP, most likely via a channel leading toward the polar headgroup region. The metabolite can escape the membrane more easily than the respective drug. DOPC chains are gray, nitrogens blue balls, phosphates brown, carbons cyan, oxygens red, and hydrogens white. The lower panel shows the free energy profile of caffeine (black) and paraxanthine (red) on a DOPC membrane. The free energy minimum and the heights of the energy barriers (water/lipid barrier ΔG^{wat} and bilayer center penetration barrier ΔG^{pen}) are labeled. The free energy profile is calculated for one leaflet and plotted symmetrically.

time (subpicosecond) resolutions. MD involves integration of simple Newtonian equations and calculates velocities of all atoms in the system from potential energy gradients.[23] The potential energy calculation is based on a simple mechanistic model known as a force field. The force field includes atomic parameters, bonds, angles, dihedrals, and charges in each molecule. The molecule is then simplified as a system of harmonic oscillators (bonds, angles, and dihedrals), and noncovalent interactions are calculated from electrostatics (applying Coulomb's law to atomic centered partial charges) and using a Lennard-Jones potential (covering dispersion and repulsion).[21,24] A variety of force fields have been developed,

dx.doi.org/10.1021/jp311802x | J. Phys. Chem. B 2013, 117, 2403−2410

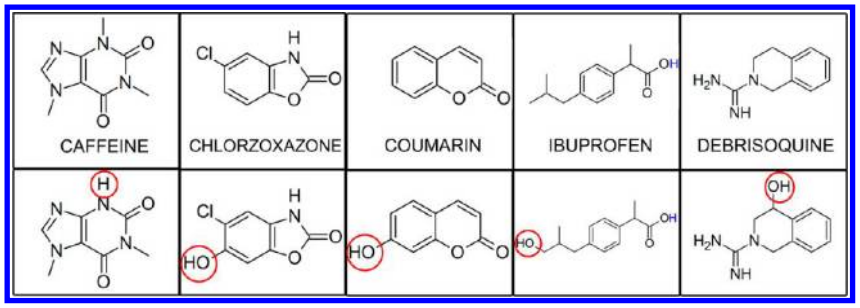

Figure 3. Structures of drugs (upper panel) and their metabolites (lower panel) showing the site of metabolism (red circles). The blue hydrogen in ibuprofen and 3-hydroxyibuprofen shows the location of deprotonation to form a charged molecule.

including all atoms, united atoms, and coarse-grained force fields.[25] The all atoms force field explicitly considers all atoms in the system, the united atoms force field (such as Berger lipid force field[26]) reduces the number of atoms in the system by uniting nonpolar hydrogens with heavy atoms (usually carbons in lipid tails), and the coarse-grained force field uses beads to represent several (usually 4) heavy atoms. The reduction of the number of atoms in the system significantly reduces computational costs, allowing longer time scales to be considered in MD simulations. It should be noted that the quality of MD simulations heavily depends on the chosen force field, and the results of MD simulation should be interpreted with care and, whenever possible, cross-validated with available experimental data.

The penetration properties of small molecules on lipid bilayers can be well described by considering the free energy (ΔG) profile along the bilayer normal, also called the potential of mean force (PMF). The free energy minimum on this profile shows the energetically most favorable position of the molecule on the bilayer. The bilayer center penetration barrier is related to the velocity of transfer of the molecule to the other monolayer (bilayer leaflet), and the water/lipid barrier reflects the affinity to the bilayer in comparison to the water environment (Figure 2). The free energy profile is usually calculated for one leaflet, and the other leaflet is plotted symmetrically. For a polar drug-like molecule, its shape is usually as follows: The free energy of an amphiphilic molecule (used in this study) in a water environment is constant when the molecule is far from the bilayer. As it moves closer to the headgroup regions, the free energy decreases (Figure 2). The polar molecules are most probably located in the water/membrane interface. As the molecule proceeds further into the lipid bilayer, the hydrophobicity of the membrane environment increases and the free energy rises, and thus the molecule must overcome an energy barrier. In the bilayer center, a local energy minimum is usually also observed;[27] the mass density of this area is slightly lower than in the outer layers, and the molecules can reside here for some time.[28]

In the present study, we analyzed the interaction of several model drugs, such as caffeine, chlorzoxazone, coumarin, ibuprofen (both its protonation forms, i.e., charged and uncharged), debrisoquine, and their corresponding major metabolites (Figure 3) with two lipid bilayers consisting of DOPC and POPG in terms of their free energy profiles along the bilayer normal. This enabled us to assess the relative comparison of the affinity of the studied compounds to the respective membranes and estimate their penetration capacities. We observed a higher affinity of drugs to the membrane compared to their CYP metabolites. Drugs and their corresponding metabolites also differed in their preferred membrane positions; that is, drugs were positioned deeper in the lipid bilayer. This observation suggests that, after the first step of removal, drugs become more hydrophilic and can leave the membrane more easily than their metabolites. We also showed another aspect of drug removal, that is, that cytochrome P450 may clean the membrane of xenobiotics. Further, we observed significant differences in the affinities to DOPC and POPG membranes, which implies that such differences can be exploited in targeting various organisms or cellular compartments.

METHODS

Model lipid bilayers were taken from the Lipidbook server.[29] DOPC bilayer was prepared and equilibrated by Siu et al.;[30] POPG was prepared by Kukol et al.[31] Both bilayers consisted of 128 lipid molecules with 64 in each leaflet. Bilayers were oriented perpendicularly to the z-axis and re-equilibrated with water and 0.154 M of NaCl. The POPG bilayer had an extra 128 Na^+ ions to achieve electroneutrality.

Several drugs and their metabolites were chosen as typical substrates for a specific CYP. We studied the stimulating alkaloid caffeine (substrate of CYP1A2), the muscle relaxant chlorzoxazone (CYP2E1), the structure base of some anticoagulants coumarin (CYP2A6), nonsteroidal analgeticum and antireumaticum ibuprofen (CYP2C9), antihypertensive debrisoquine (CYP2D6), and their respective major metabolites paraxanthine, 6-hydroxychlorzoxazone, 7-hydroxycoumarin, 3-hydroxyibuprofen, and 4-hydroxydebrisoquine, respectively. As ibuprofen bears a titratable carboxy group, we analyzed both protonation states (protonated $-COOH$ and unprotonated negatively charged $-COO^-$) for it and the respective metabolite.

Structures and topologies of drugs and metabolites were built using the PRODRG2Beta[32] server. The atom types and bond parameters assigned by PRODRG are compatible with the lipid force field, but the assigned partial charges for hydrophobic groups make these groups too hydrophilic, and therefore these charges are not compatible with GROMOS force fields.[33] The atomic partial charges were derived using the RESP[34] (restraint electrostatic potential) procedure from an electrostatic potential calculated on a B3LYP/cc-pVDZ level of theory on structures equilibrated on the same level of theory in Gaussian 03.[35] The RESP fit was carried out using Antechamber from the AMBER 11 software package.[36] Recently, we have shown that the RESP partial charges provide free energy profiles along bilayer normal, reasonably agreeing with available experimental data.[28]

dx.doi.org/10.1021/jp311802x | J. Phys. Chem. B 2013, 117, 2403−2410

Table 1. Free Energy Profiles and Hydration Free Energies (ΔG^{hyd}) of the Studied Molecules[a]

			DOPC					POPG				
	log P	ΔG^{hyd}, kcal/mol	P, nm	P_{rel}, %	ΔG^{pen}, kcal/mol	ΔG^{wat}, kcal/mol	pK_m	P, nm	P_{rel}, %	ΔG^{pen}, kcal/mol	ΔG^{wat}, kcal/mol	pK_m
caffeine	−0.1[b]	−8.8	1.6	78	4.1 ± 0.6	5.7 ± 0.1	−2.8	1.6	101	7.6 ± 0.8	6.3 ± 0.1	−3.2
paraxanthine	−0.2[b]	−11.2	2.1	99	8.0 ± 0.1	4.9 ± 0.1	−2.2	1.5	96	6.9 ± 0.1	5.1 ± 0.3	−2.4
chlorzoxazone	2.2[b]	−8.4	1.5	72	8.2 ± 1.0	8.9 ± 0.8	−5.2	1.0	66	4.7 ± 0.4	8.1 ± 0.5	−4.2
6-hydroxy-chlorzoxazone	1.7	−11.5	1.6	75	8.3 ± 0.7	8.2 ± 0.4	−4.5	1.7	108	8.9 ± 0.8	7.0 ± 0.8	−3.5
coumarin	1.4[b]	−6.0	1.3	63	3.0 ± 0.2	6.7 ± 0.2	−3.5	1.4	88	3.6 ± 0.2	5.3 ± 0.1	−2.7
7-hydroxy-coumarin	1.6[b]	−10.5	1.6	78	4.8 ± 1.0	2.9 ± 1.0	−1.0	1.6	97	4.1 ± 0.6	4.2 ± 0.6	−2.0
ibuprofen	3.7[b]	−11.3	1.4	65	6.8 ± 1.5	7.7 ± 0.1	−4.4	1.6	100	5.0 ± 0.2	3.1 ± 0.1	−1.2
3-hydroxy-ibuprofen	1.7	−17.5	1.5	70	8.3 ± 0.1	3.0 ± 1.0	−1.3	1.4	86	5.2 ± 0.1	2.2 ± 1.4	−0.5
debrisoquine	0.1[b]	−18.3	1.7	79	5.6 ± 1.0	4.8 ± 0.7	−2.3	1.4	86	4.6 ± 0.2	2.5 ± 0.5	−0.7
4-hydroxy-debrisoquine	−0.7	−18.3	1.6	77	7.0 ± 0.7	1.8 ± 0.3	−0.2	1.8	113	12.5 ± 2.3	3.5 ± 0.7	−0.9

[a]The positions of the minima (P) show the most probable location of the molecule in the membrane. The relative position (P_{rel}) shows the ratio of the position of the free energy minimum P and the position of phosphates (100% means that the molecule is at the phosphate "plane"; higher and lower numbers indicate positions above and below the phosphates), ΔG^{pen} and ΔG^{wat} are the bilayer center penetration and water/lipid barrier, respectively, while pK_m is the negative logarithm of the molar ratio K_m of the molecule between the lipid and water phase. [b]Experimental values of octanol/water partition coefficients.

All molecular dynamics (MD) simulations were performed using the GROMACS 4.0.7 software package[37] with a Berger lipid force field[26] based on the GROMOS 53a6 force field.[38] This force field unites nonpolar hydrogens with corresponding carbons and reduces the number of simulated atoms in long hydrocarbon chains present in lipids. However, this simplification is likely to bias the diffusion coefficient calculation and leads to its higher values.[39] The simulations were carried out with time steps of 2 fs. The periodic boundary conditions were applied in all directions, electrostatics was solved by the particle-mesh Ewald method,[40] van der Waals cutoff was set at 1 nm, and bond constraints were determined by LINCS algorithm.[41] We used V-rescale temperature coupling[42] to 310 K and Berendsen anisotropic pressure coupling[43] to 1 bar with a time constant of 10 ps and compressibility of 4.5×10^{-5} bar^{-1}.

The free energy profile can be calculated from biased simulations using various techniques, such as umbrella sampling,[44,45] z-constraint,[13,27,46−49] metadynamics,[50,51] and others.[52] For consistency with our previous study,[4] we here used the umbrella sampling method. Umbrella sampling applies a harmonic potential around the starting position of a molecule (at a specific depth in a bilayer). The applied force on the molecule is proportional to the square of the displacement from the original distance of the two groups (molecule and lipid bilayer), and the free energy profile can then be calculated from eq 1:[23,53]

$$\Delta G(z) = -RT \ln P(z) + U(z) \quad (1)$$

Molecules of substrates and metabolites were inserted into the simulation box containing a hydrated lipid bilayer with SPCE water model,[54] and a short 0.5 ns long simulation was executed to relax water molecules and the simulation box. The initial structures for umbrella simulations were obtained using the following two methods: either the molecule was free to go anywhere by itself (referred to as UF) or the center of mass of the molecule was pulled into the bilayer (UP). Frames separated by 0.1 ± 0.02 nm were chosen from the trajectories, and the frames with the lowest potential energies were selected as initial structures. Usually these two approaches were combined; the free simulation was used to generate as many starting frames as possible and then followed by a pulling simulation (see Supporting Information Table S1).

The initial structures were subsequently used in the umbrella sampling simulation. The initial distance in the umbrella simulation was restrained by a harmonic force of 2000 kJ mol^{-1} nm^{-2} (477.9 kcal mol^{-1} nm^{-2}). Each window was simulated for 10.25 ns. The first 2250 ps was taken as pre-equilibration of the system. The free energy profiles were analyzed, and the convergence of energy barriers and positions of minima was monitored. The simulations of molecules that did not show stable values of energy barriers' heights and positions of minima were prolonged (see Table S1 and Figures S1 and S2 in the Supporting Information). The free energy profile was calculated by the weighted histogram analysis method[44] (WHAM) using g_wham[55] from the GROMACS software package. The start of the z axis was set to the middle of the membrane.

The free energy profiles of ibuprofen and 3-hydroxyibuprofen were calculated from profiles of their charged and uncharged forms. As the pK_A of ibuprofen is 4.44, its free energy in water was shifted by 3.5 kcal/mol (the same value was used as an estimate for 3-hydroxyibuprofen). The lowest energies in the free energy profiles were then used to estimate the preferential form of the molecules in the specified positions.

The hydration free energy ΔG^{hyd} was calculated by the Bennett acceptance ratio (BAR) method[56] with $\Delta\lambda = 0.05$. A simulation box with an SPCE[54] water model (∼500 water molecules) and one molecule of drug/metabolite was prepared and equilibrated. The BAR method calculates the free energy of change when a target molecule "appears" in a solvent. Each (total 21 for each molecule) simulation was executed for 200 ps, with the first 100 ps used for equilibration. The total ΔG^{hyd} was integrated using g_bar in the software package GROMACS 4.5.1.

The distribution coefficients of drugs and their metabolites between a membrane and water phase can be calculated from the free energy profile along the membrane normal. Individual distribution coefficients at position z' in the membrane, $D(z')$, were given by the free energy difference to the reference value of free energy in water, where ΔG was set to 0 kcal/mol. The global distribution coefficient, D, for a given molecule was

dx.doi.org/10.1021/jp311802x | J. Phys. Chem. B 2013, 117, 2403−2410

integrated from the individual $D(z')$ along both membrane leaflets (eq 2):

$$D = \frac{c_{\text{membrane}}}{c_{\text{water}}} = 2 \cdot \int_0^z e^{-\Delta G(z\prime)/RT}\, dz' \quad (2)$$

where z is one-half of the bilayer thickness (2.5 nm), $\Delta G(z')$ is the free energy of the molecule at depth z', T is the thermodynamic temperature, and R is the universal gas constant.

To obtain not only the concentration ratio between lipid bilayer and water but also the approximate molar ratio K_m, the volume ratio between water and lipids has to be taken into account. Lipids form about 5% of the mass of human cells, whereas water accounts for as much as 70%;[19] the densities of both phases are approximately the same. The approximate molar ratio K_m of a drug between lipids (n_{membrane}) and water (n_{water}) in the human body can then be estimated from eq 3:

$$K_m = \frac{n_{\text{membrane}}}{n_{\text{water}}} = D \cdot \frac{V_{(\text{membrane})}}{V_{(\text{water})}} \quad (3)$$

where $V_{(\text{membrane})}/V_{(\text{water})}$ is the volume ratio (5/70). Values are usually reported as pK_m.

Octanol/water partition coefficients (log P) were adopted from experimental values taken from DrugBank[57] whenever possible, and other values were taken from the ChemSpider[58] Web site.

The heights of energy barriers were obtained from the free energy profiles along with the positions of the center-of-mass of the molecule in the free energy minima P and the relative position of the energy minimum with respect to the positions of phosphates P_{rel}. The mean values for drugs, metabolites, or all molecules on each bilayer were taken as the median of the obtained values.

RESULTS AND DISCUSSION

Free Energy Profiles Show Typical Behavior of Amphiphilic Drug-like Molecules on Lipid Bilayers. The free energy profiles show the positions of minima, where the molecules are likely to concentrate. The free energy profiles of molecules on a DOPC bilayer (Figure 2 and Table 1) decrease from the water phase to region 2 or 3, where typically one energy minimum is located. One shallow local minimum appears in the middle of the bilayer, where the overall density of the bilayer drops (Figure 1). These profiles indicate that the studied molecules can spontaneously enter the lipid bilayer. The molecules may concentrate in the lipid phase, as is also apparent by the negative pK_m values. The molecules then preferentially stay close to their minima, which are localized in regions 2 and 3. It should be noted that the entrances of active site access channels of CYP enzymes most likely stay in the same regions.[4,59,60] Here, the drugs can be taken up by CYP to be modified.

The free energy profiles of molecules on a POPG bilayer are similar to those on DOPC bilayers. They display a deep energy minimum in regions 2 or 3. On the other hand, a local energy minimum in the middle of the POPG bilayer is rare. The overall density of the POPG bilayer with respect to DOPC is lower. However, there is only a small decrease in mass density in the POPG bilayer center, and therefore the molecules do not prefer to stay in the bilayer center. Because of the small decrease in mass density, POPG does not have a region near the bilayer center characterized by rapid lateral diffusion in contrast to DOPC.

Heterogeneity of Membrane Environment Reduces the Correlation of Partitioning in Octanol/Water and Lipids/Water Environments. We have compared the calculated parameters of the free energy profile with the octanol/water partition coefficient (log P), which is widely used to predict a drug bioavailability. We observed a rather poor correlation (correlation coefficient below 0.3, which is not statistically significant at level of significance $\alpha = 0.05$, indeed) for positioning, partitioning, and consequently also ΔG^{wat} on DOPC, and no correlation on POPG bilayer (Figure S3). The low correlation between log P and ΔG^{wat} values on DOPC can be explained by a more complex structure of the lipid bilayer. The outer parts of the membrane bilayer are more polar than octanol/water surface; therefore, the polar molecules are more concentrated on membranes than they are on octanol/water interface. No correlation of calculated free energy profile properties with log P was observed on POPG, which might be explained by the fact that the molecules were preferentially located on the bilayer/water interface, where about 20% of mass was formed by water. The octanol/water partition coefficient can therefore reflect partition properties on some membrane types,[61,62] but cannot be straightforwardly used on all types of membranes and all molecules.

Drugs Have Higher Affinity to the Bilayer than Corresponding Metabolites. The free energy profiles show that the studied drugs have a higher affinity to the lipid bilayer and are located deeper in the bilayers than are the corresponding metabolites. It is supported by the fact that ΔG^{hyd} of the drugs is higher than the corresponding value of the metabolites, and thus the drugs are more hydrophobic than their respective metabolites. The drugs are also on average 0.2 nm deeper in the bilayer than their metabolites (Figures 2 and 4, and Table 1). The bilayer center penetration barrier ΔG^{pen} for drugs is typically lower than that of the metabolites (2.4 kcal/mol on DOPC and 2.2 kcal/mol on POPG). On the other hand, the water/lipid barrier ΔG^{wat} is higher for the drugs than the metabolites (3.7 kcal/mol on DOPC and 1.1 kcal/mol on POPG). The higher membrane affinity of the drugs is clearly visible from the molar ratio pK_m of the molecule in the membrane and water, with the exception of debrisoquine on POPG (Table 1 and Figure 5).

The drugs' metabolites have different charge distributions, and therefore exhibit different orientations on the lipid bilayers. The drugs have polar group(s) located on one side of the molecule (with the exception of caffeine) and are usually oriented with these polar groups pointing toward the polar lipid heads. The metabolites are typically hydroxylated on the other side of the molecule (with the exception of paraxanthine, which is demethylated), and therefore are oriented more parallel to the bilayer.

Implications for Drug Metabolism by Cytochromes P450 (CYP). As mentioned before, the studied drugs concentrate in the lipid bilayer, and their preferred positions correspond with CYP active site access channel influxes (Figure 5). The CYP metabolized drugs are believed to leave the CYPs active sites via egress tunnels that open further from the bilayer center close to the polar headgroup region. It is worth noting that the metabolites can leave the bilayer more easily, as their affinities to the membranes (represented by pK_m and ΔG^{wat}) are lower than the respective affinities of drugs (cf., Figure 5 and Table 1).

dx.doi.org/10.1021/jp311802x | J. Phys. Chem. B 2013, 117, 2403−2410

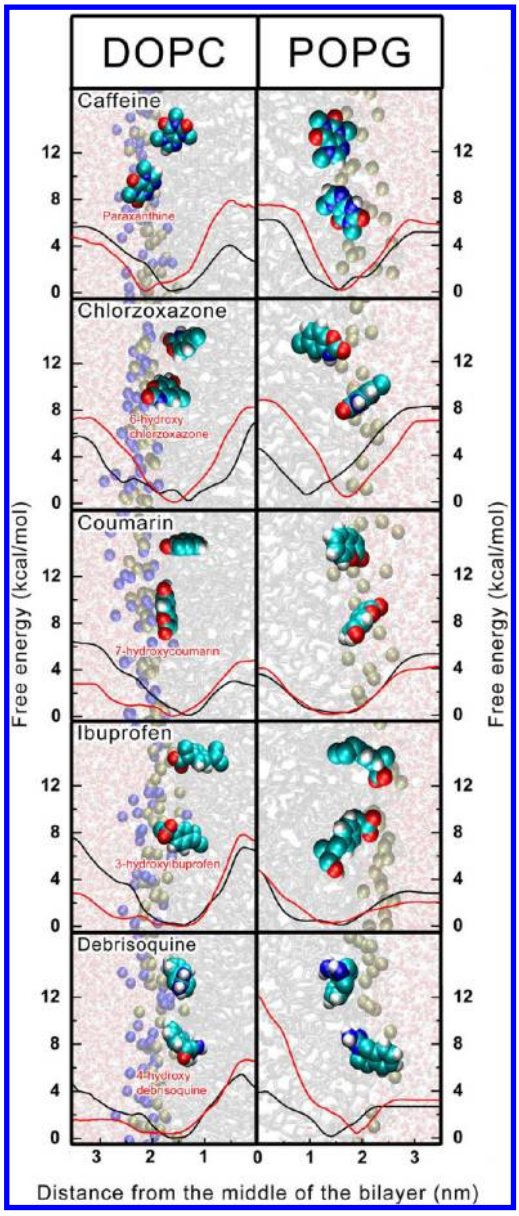

Figure 4. The free energy profiles of the studied molecules in DOPC (left) and POPG (right) bilayers. The free energy profile of the drug (the upper molecule of each box) is plotted in black, whereas the free energy profile of the CYP metabolite (the lower molecule) is in red. The structures of the drugs and their metabolites are shown in their energy minima. The drugs are located deeper in the bilayer than the corresponding metabolites and usually have higher affinities to the lipid bilayer. DOPC and POPG chains are shown in gray, nitrogens are represented as blue balls, phosphates brown, carbons cyan, oxygens red, and hydrogens white.

Molecules Pass through POPG Bilayer More Easily. The molecules on POPG are usually located closer to the water environment and are bound more weakly than the molecules on DOPC. The POPG bilayer is thinner, but the mean relative position of the molecules on POPG is about 20% closer to the polar headgroup region than on the DOPC bilayer. Molecules on POPG are located in an area where the overall mass is formed by about 20% of water, whereas the mean position of molecules on DOPC is in an area where water comprises only about 2% of the overall mass. This also reduces the water/lipid barrier ΔG^{wat} on POPG as its median is 0.6 kcal/mol lower for

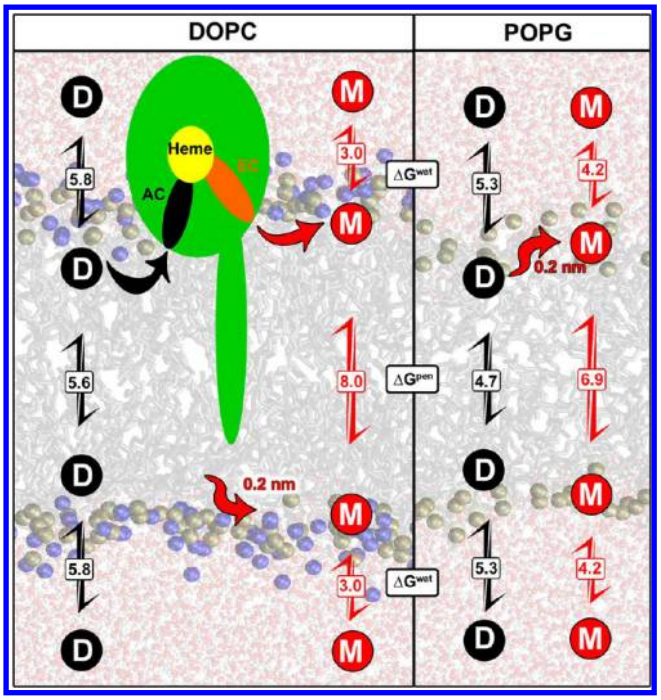

Figure 5. Proposed scheme of drug (D) and metabolite (M) penetration through the DOPC (left panel) and POPG (right panel) bilayers with medians of the obtained energy barriers and proposed scheme of the drug entering and leaving cytochrome P450 (CYP – green object on the left panel), which is anchored to the membrane of endoplasmic reticulum. The water/lipid barrier ΔG^{wat} is higher and the bilayer center penetration barrier ΔG^{pen} is lower for the drugs than for metabolites. The metabolites are located 0.2 nm further from the bilayer center than the drugs in both cases. The overall energy barriers are lower on POPG than on DOPC. The drugs are believed to enter CYP by access channel (AC – in black), it is metabolized in the active site above the heme (in yellow), and leaves CYP via egress channel (EC – orange) as a metabolite. The egress channel opens close to the water region.

molecules on POPG than on DOPC. The bilayer center penetration barrier ΔG^{pen} is also on average 1.8 kcal/mol lower for molecules on POPG. The affinity to the lipid bilayer is higher for molecules on DOPC than on POPG, and therefore the molecules prefer to concentrate in DOPC lipid bilayers. However, small drug-like molecules seem to pass through the POPG bilayer more easily than through DOPC. It should be noted that we used a limited number of molecules in the study and the results gained have to be interpreted with caution as comparison of the data between single pairs of other molecules may lead to different conclusions. However, it is known that membranes of mammals consist mostly of PC, whereas bacterial membranes contain large amounts of negatively charged PG. Thus, the easier penetration and lower concentration of small drugs on POPG membranes could be used in targeted drug delivery.

CONCLUSION

Here, we studied the interaction of five drugs and their respective CYP metabolites with lipid bilayers in terms of their free energy profiles across two prototypical lipid bilayers consisting of DOPC and POPG. We showed that the behavior of the studied drugs and their metabolites on lipid bilayers differed in numerous ways. The drugs (which are more hydrophobic molecules than their respective metabolites)

dx.doi.org/10.1021/jp311802x | J. Phys. Chem. B 2013, 117, 2403–2410

exhibited higher water/lipid free energy barriers ΔG^{wat}, and therefore a higher affinity to the lipid bilayers than the metabolites. Furthermore, the drugs can penetrate the membrane with lower energy barriers ΔG^{pen} than their respective metabolites. The results imply that the respective metabolites are generally more weakly bound to the membrane and more likely to stay in the cytosol than the drugs. This behavior may have implications for the metabolism of the studied drugs by CYPs. As the drugs prefer to stay in the membrane, they are likely to enter the CYP buried active site via access channels from the membrane. On the other hand, the generally more polar substrates may leave the active site by egress channels pointing toward the membrane surface or cytosol.

Furthermore, the results show that the behavior of drug-like molecules differs on different lipid bilayers. The free energy profiles indicate that the ratio of the number of molecules in the membrane to that in water is slightly higher for DOPC than for POPG. Therefore, the drugs are likely to concentrate more on DOPC bilayers. However, the energy barriers are lower on POPG, and therefore penetration through POPG bilayers seems to be easier. As the penetration through the membrane is crucial for reaching the biological target and also some drug effects are based on the change of bilayer properties as the drugs concentrate in membranes, we believe that such information, along with knowledge of membrane composition, would be useful for drug targeting.

■ ASSOCIATED CONTENT

Supporting Information

Detailed information on simulations. This material is available free of charge via the Internet at http://pubs.acs.org.

■ AUTHOR INFORMATION

Corresponding Author

*Phone: +420 585634769 (K.B.); +420 585634756 (M.O.). Fax: +420 585634761 (M.O.). E-mail: karel.berka@upol.cz (K.B.); michal.otyepka@upol.cz (M.O.).

Notes

The authors declare no competing financial interest.

■ ACKNOWLEDGMENTS

We acknowledge the support by the Operational Program Research and Development for Innovations − European Regional Development Fund (project CZ.1.05/2.1.00/03.0058 of the Ministry of Education, Youth and Sports of the Czech Republic) and the Operational Program Education for Competitiveness − European Social Fund (projects CZ.1.07/2.3.00/20.0017 and CZ.1.07/2.3.00/20.0058). This work was also supported by the Grant Agency of the Czech Republic through the P208/12/G016, 303/09/1001, 203/09/H046, and P303/12/P019 projects and by a student project PrF_2012_028.

■ REFERENCES

(1) Seydel, J. K.; Wiese, M. In *Drug-Membrane Interactions: Analysis, Drug Distribution, Modeling*; Mannhold, R., Kubinyi, H., Folkers, G., Eds.; Wiley-VCH Verlag GmbH: Weinheim, 2002.
(2) Peetla, C.; Stine, A.; Labhasetwar, V. *Mol. Pharmaceutics* **2009**, *6*, 1264−1276.
(3) Lúcio, M.; Lima, J. L. F. C.; Reis, S. *Curr. Med. Chem.* **2010**, *17*, 1795−1809.
(4) Berka, K.; Hendrychová, T.; Anzenbacher, P.; Otyepka, M. *J. Phys. Chem. A* **2011**, *115*, 11248−11255.
(5) Nagar, S.; Korzekwa, K. *Drug Metab. Dispos.* **2012**, *40*, 1649−52.
(6) Orsi, M.; Essex, J. W. In *Molecular Simulations and Biomembranes*; Sansom, M. S. P., Biggin, P. C., Eds.; Royal Society of Chemistry: UK, 2010; pp 76−90.
(7) Ayrton, A.; Morgan, P. *Xenobiotica* **2001**, *31*, 469−497.
(8) Shitara, Y.; Horie, T.; Sugiyama, Y. *Eur. J. Pharm. Sci.* **2006**, *27*, 425−146.
(9) Giacomini, K. M.; Huang, S.-M.; Tweedie, D. J.; Benet, L. Z.; Brouwer, K. L. R.; Chu, X.; Dahlin, A.; Evers, R.; Fischer, V.; Hillgren, K. M.; et al. *Nat. Rev. Drug Discovery* **2010**, *9*, 215−236.
(10) Mouritsen, O. G.; Jorgensen, K. *Pharm. Res.* **1998**, *15*, 1507−1519.
(11) Black, S. D. *FASEB J.* **1992**, *6*, 680−685.
(12) Košinová, P.; Berka, K.; Wykes, M.; Otyepka, M.; Trouillas, P. *J. Phys. Chem. B* **2012**, *116*, 1309−18.
(13) Orsi, M.; Essex, J. W. *Soft Matter* **2010**, *6*, 3797−3808.
(14) Kirjavainen, M.; Monkkonen, J.; Saukkosaari, M.; Valjakka-koskela, R.; Kiesvaara, J.; Urtti, A. *J. Controlled Release* **1999**, *58*, 207−214.
(15) Cohen, Y.; Bodner, E.; Richman, M.; Afri, M.; Frimer, A. A. *Chem. Phys. Lipids* **2008**, *155*, 98−113.
(16) MacCallum, J. L.; Tieleman, D. P. *J. Am. Chem. Soc.* **2006**, *128*, 125−130.
(17) Cooper, G. M. *The Cell, A Molecular Approach*; Sinauer Associates: Sunderland, MA, 2000.
(18) Yeagle, P. L. *Encyclopedia of Life Sciences (ELS)*; Joh Wiley & Sons, Ltd.: Chichester, 2009.
(19) Alberts, B.; Johnson, A.; Lewis, J.; Raff, M.; Roberts, K.; Walter, P. *Molecular Biology of the Cell*, 4th ed.; Garland Science: New York, 2002.
(20) Otyepka, M.; Skopalík, J.; Anzenbacherová, E.; Anzenbacher, P. *Biochim. Biophys. Acta* **2007**, *1770*, 376−389.
(21) Dowhan, W. *Annu. Rev. Biochem.* **1997**, *66*, 199−232.
(22) Marrink, S.-J.; Berendsen, H. J. C. *J. Phys. Chem.* **1994**, *98*, 4155−4168.
(23) Van Der Spoel, D.; Lindahl, E.; Hess, B.; Groenhof, G.; Mark, A. E.; Berendsen, H. J. C. *J. Comput. Chem.* **2005**, *26*, 1701−1718.
(24) Zgarbová, M.; Otyepka, M.; Šponer, J.; Hobza, P.; Jurečka, P. *Phys. Chem. Chem. Phys.* **2010**, *12*, 10476−10493.
(25) Schlick, T. *Molecular Modeling and Simulation: An Interdisciplinary Guide*, 2nd ed.; Springer: New York, 2010.
(26) Berger, O.; Edholm, O.; Jahnig, F. *Biophys. J.* **1997**, *72*, 2002−2013.
(27) Bemporad, D.; Essex, J. W.; Luttmann, C. *J. Phys. Chem. B* **2004**, *108*, 4875−4884.
(28) Paloncýová, M.; Berka, K.; Otyepka, M. *J. Chem. Theory Comput.* **2012**, *8*, 1200−1211.
(29) Domański, J.; Stansfeld, P. J.; Sansom, M. S. P.; Beckstein, O. *J. Membr. Biol.* **2010**, *236*, 255−258.
(30) Siu, S.; Vácha, R.; Jungwirt, P.; Böckmann, R. A. *J. Chem. Phys.* **2008**, *128*, 125103.
(31) Kukol, A. *J. Chem. Theory Comput.* **2009**, *5*, 615−626.
(32) Schüttelkopf, A. W.; Van Aalten, D. M. F. *Acta Crystallogr., Sect. D: Biol. Crystallogr.* **2004**, *60*, 1355−1363.
(33) Lemkul, J. A.; Allen, W. J.; Bevan, D. R. *J. Chem. Inf. Model.* **2010**, *50*, 2221−2235.
(34) Cieplak, P.; Caldwell, J.; Kollman, P. *J. Comput. Chem.* **2001**, *22*, 1048−1057.
(35) Frisch, M. J.; Trucks, G. W.; Schlegel, H. B.; Scuseria, G. E.; Robb, M. A.; Cheeseman, J. R.; Montgomery, J. A., Jr.; Vreven, T.; Kudin, K. N.; Burant, J. C.; et al. *Gaussian 03*, revision E.01; Gaussian, Inc.: Wallingford, CT, 2004.
(36) Case, D. A.; Darden, T. A.; Cheatham, T. E., III; Simmerling, C. L.; Wang, J.; Duke, R. E.; Luo, R.; Walker, R. C.; Zhang, W.; Merz, K. M.; et al. *AMBER 11*; University of California: San Francisco, CA, 2010.

(37) Hess, B.; Kutzner, C.; Van der Spoel, D.; Lindahl, E. *J. Chem. Theory Comput.* **2008**, *4*, 435−447.
(38) Oostenbrink, C.; Soares, T. A.; Van der Vegt, N. F. A.; Van Gunsteren, W. F. *Eur. Biophys. J.* **2005**, *34*, 273−284.
(39) Shinoda, W.; Mikami, M.; Baba, T.; Hato, M. *J. Phys. Chem. B* **2004**, *108*, 9346−9356.
(40) Darden, T.; York, D.; Pedersen, L. *J. Chem. Phys.* **1993**, *98*, 10089−10092.
(41) Hess, B.; Bekker, H.; Berendsen, H. J. C.; Fraaije, J. G. E. M. *J. Comput. Chem.* **1997**, *18*, 1463−1472.
(42) Bussi, G.; Donadio, D.; Parrinello, M. *J. Chem. Phys.* **2007**, *126*, 014101.
(43) Berendsen, H.; Postma, J.; Vangunsteren, W.; Dinola, A.; Haak, J. *J. Chem. Phys.* **1984**, *81*, 3684−3690.
(44) Kumar, S.; Rosenberg, J.; Bouzida, D.; Swensen, R. H.; Kollman, P. A. *J. Comput. Chem.* **1992**, *13*, 1011−1021.
(45) Torrie, G. M.; Calleau, J. P. *J. Comput. Phys.* **1997**, *23*, 187−199.
(46) Boggara, M. B.; Krishnamoorti, R. *Biophys. J.* **2010**, *98*, 586−595.
(47) Bemporad, D.; Luttmann, C.; Essex, J. W. *Biophys. J.* **2004**, *87*, 1−13.
(48) Marrink, S. J.; Berendsen, H. J. C. *J. Phys. Chem.* **1996**, *100*, 16729−16738.
(49) Orsi, M.; Sanderson, W. E.; Essex, J. W. *J. Phys. Chem. B* **2009**, *113*, 12019−12029.
(50) Zhang, Y.; Voth, G. A. *J. Chem. Theory Comput.* **2011**, *7*, 2277−2283.
(51) Laio, A.; Parrinello, M. *Proc. Natl. Acad. Sci. U.S.A.* **2002**, *99*, 12562−12566.
(52) Roux, B. *Comput. Phys. Commun.* **1995**, *91*, 275−282.
(53) Xiang, T.-X.; Anderson, B. D. *Adv. Drug Delivery Rev.* **2006**, *58*, 1357−1378.
(54) Berendsen, H. J. C.; Postma, J. P. M.; Gunsteren, W. F.; van Hermans, J. In *Intermolecular Forces*; Pullman, B., Ed.; Reidel Publishing Co.: Dordrecht, The Netherlands, 1981; pp 331−338.
(55) Hub, J. S.; Groot, B. L. De; Spoel, D. Van Der *J. Chem. Theory Comput.* **2010**, *6*, 3713−3720.
(56) Bennett, C. *J. Comput. Phys.* **1976**, *22*, 245−268.
(57) DrugBank; www.drugbank.ca (accessed Jan 28, 2013).
(58) ChemSpider − The free chemical database; www.chemspider.com (accessed Jan 25, 2013).
(59) Cojocaru, V.; Balali-Mood, K.; Sansom, M. S. P.; Wade, R. C. *PLoS Comput. Biol.* **2011**, *7*, e1002152.
(60) Denisov, I. G.; Shih, Y.; Sligar, S. G. *J. Inorg. Biochem.* **2012**, *108*, 150−8.
(61) Vaes, W. H.; Ramos, E. U.; Hamwijk, C.; Van Holsteijn, I.; Blaauboer, B. J.; Seinen, W.; Verhaar, H. J.; Hermens, J. L. *Chem. Res. Toxicol.* **1997**, *10*, 1067−72.
(62) Vaes, W. H. J.; Verhaar, H. J. M.; Cramer, C. J.; Hermens, J. L. M. *Chem. Res. Toxicol.* **1998**, *11*, 847−854.